



# CHORUS

This is the accepted manuscript made available via CHORUS. The article has been published as:

## Two-dimensional interaction of spin chains in the Si(553)- Au nanowire system

B. Hafke, T. Frigge, T. Witte, B. Krenzer, J. Aulbach, J. Schäfer, R. Claessen, S. C. Erwin,  
and M. Horn-von Hoegen

Phys. Rev. B **94**, 161403 — Published 18 October 2016

DOI: [10.1103/PhysRevB.94.161403](https://doi.org/10.1103/PhysRevB.94.161403)

# Two-Dimensional Interaction of Spin Chains in the Si(553)-Au Nanowire System

B. Hafke,<sup>1,\*</sup> T. Frigge,<sup>1</sup> T. Witte,<sup>1</sup> B. Krenzer,<sup>1</sup> J. Aulbach,<sup>2</sup>  
J. Schiøtzer,<sup>2</sup> R. Claessen,<sup>2</sup> S.C. Erwin,<sup>3</sup> and M. Horn-von Hoegen<sup>1</sup>

<sup>1</sup>*Department of Physics and Center for Nanointegration (CENIDE),  
University of Duisburg-Essen, 47057 Duisburg, Germany*

<sup>2</sup>*Röntgen Research Center for Complex Material Systems (RCCM),  
University of Wüzzerzburg, 97074 Wüzzerzburg, Germany*

<sup>3</sup>*Center for Computational Materials Science, Naval Research Laboratory, Washington, DC 20375, United States*

(Dated: August 11, 2016)

Adsorption of Au on Si(553) results in the self-assembly of highly ordered step arrays of one-dimensional (1D) Au atomic wires along the step direction. Charge transfer from the terrace to the step edge causes that every third Si atom at the step edge exhibits a partially filled dangling bond hosting a single fully spin polarized electron which forms in an ordered 1D spin chain along the step. The interstep correlation of this 3-fold periodicity in neighboring Si step edges and the geometry of the unit cell has been determined by means of high-resolution spot profile analysis low energy electron diffraction, scanning tunneling microscopy, and density-functional theory. While the 2-fold periodicity of the Au wires exhibits a weak interwire interaction leading to streaks in the diffraction pattern, the correlation of the Si step edge atoms is a by far stronger interaction, resulting in clear spots. The corresponding unit cell spanned by the threefold ordered step edge atoms can be described as a centered structure which is magnetically frustrated and may stabilize a (2D) quantum spin liquid.

PACS numbers: 68.35.Bs, 68.47.Fg

The assembly of single atoms into chains has attracted a lot of attention during the last years<sup>1</sup>, because of the wealth of intriguing phenomena peculiar to the world of one dimension. Such atomic wire systems exhibit properties like intrinsic electronic and structural instabilities, resulting in the formation of charge density waves or spin density waves, depending on the interaction strength between electron system and lattice. In reality, such one-dimensional metallic atomic wire systems can be realized through self-assembly during the adsorption of metal atoms on perfectly aligned atomic terraces of vicinal Si surfaces<sup>2-5</sup>.

One of the most spectacular findings in such atomic wire systems is the existence of highly ordered 1D arrays of spins associated with the dangling-bond orbitals along a row of Si step-edge atoms<sup>5-10</sup>. Employing the miscut of the surface, the interwire coupling can easily be adjusted and 2D magnetic ordering of the spins may become possible at low temperatures. Here we raise the question of the geometry and the magnetic long range ordering versus possible magnetic frustration induced by the increasing 2D interaction. We use a prototypical atomic wire system, namely the Si(553) surface decorated with rows of Au atoms, to answer the question by means of high resolution low-energy electron diffraction (LEED), scanning tunneling microscopy (STM), and density-functional theory (DFT).

The Si(553) surface can be described as equally spaced (111) terraces separated by a single atomic step height of  $a_{\text{step}} = 3.14 \text{ \AA}$ , and a distance between steps of  $a_{\perp} = 14.8 \text{ \AA}$ . The atomic distance in the  $[1\bar{1}0]$  direction, i.e., along the steps, is  $a_0 = 3.84 \text{ \AA}$ . Au adsorption leads to the formation of linear chains, whose 1D metal-

lic nature has been confirmed in several electronic band structure studies<sup>11-14</sup>. Early works on Si(553) assumed a Au coverage of 0.25 ML<sup>11,15,16</sup>, corresponding to a single chain of Au atoms along the terraces. In a X-ray diffraction (XRD) study Ghose *et al.* proposed the formation of an Au double row decorating the step edges in the Si(553)-Au system<sup>17</sup> with an Au coverage of 0.5 ML. STM simulations, however, seemed to be in good agreement with a single atomic Au row in the middle of the terrace<sup>15,18</sup>. Finally, diffraction experiments also gave strong favor to an Au coverage of 0.5 ML<sup>19,20</sup>. Well below room temperature electron diffraction patterns show a twofold ( $\times 2$ ), and a threefold ( $\times 3$ ) periodicity along the steps, respectively<sup>12,19,21</sup>. The former is assigned to the dimerization of the Au double row along the steps<sup>22</sup>. An *ab-initio* calculation confirmed that the dimerized double row Au chain in the middle of the terrace and a single honeycomb-like graphitic strip of Si atoms at the step edge is energetically most favorable<sup>22</sup>, which is consistent with STM<sup>9,12,13,15,23,24</sup> and XRD<sup>20</sup> studies. DFT calculations taking into account spin polarization led to the most recent structure model<sup>6</sup> referred to as *original* in the following. Every third Si step edge atom of the honeycomb-like strip carries a half-filled electron orbital with corresponding lower density, leading to the intriguing prediction that these Si atoms are intrinsically fully spin polarized. The coupling between neighboring spin polarized Si atoms along the steps is proposed to be antiferromagnetic, while it is ferromagnetic across the steps. The fingerprint of these spin chains is a distinct unoccupied electronic state several tenth of eV above the Fermi level, as predicted by DFT<sup>6</sup> and detected in scanning tunneling spectroscopy (STS) studies<sup>8-10</sup>. STM images

taken at a tunneling bias sensitive to that characteristic DOS show the pronounced  $\times 3$  periodicity<sup>9</sup>.

Here, we present experimental evidence that the *original* structure model exhibits a unit cell which has to be modified to correctly describe the  $\times 2$ - and  $\times 3$  periodicities found in the LEED pattern. The long-range order of adjacent Si step edge atoms perpendicular to the steps is exceptionally strong. From a detailed analysis of the diffraction pattern, which is representative for  $\text{mm}^2$  surface areas as well as the corresponding STM images reflecting the local morphology, two questions regarding the surface structure can be answered: The first is the solution of the geometry of the unit cell and second its impact on the magnetic ordering when taking the proposed spin ordered ground state as a basis.

The experiments were performed under ultra-high vacuum conditions (UHV) at a base pressure of  $p \approx 2 \times 10^{-10}$  mbar. A *n*-type Si(553) substrate (phosphorus doped,  $0.01 \text{ } \Omega\text{cm}$ ) mounted on a liquid nitrogen cryostat was used. After cleaning via direct current heating up to  $1250^\circ\text{C}$  in several short flash-anneal cycles, the sample was held at an elevated temperature of  $650^\circ\text{C}$ . Au was deposited from an electron beam-heated graphite crucible<sup>25</sup> followed by a post annealing step at  $850^\circ\text{C}$ <sup>9</sup>. Subsequently the sample was rapidly cooled to liquid nitrogen temperatures. The surface morphology was determined with a spot profile analysis low-energy electron diffraction (SPA-LEED) instrument<sup>26,27</sup>. LEED patterns were taken at a temperature of 80 K and an electron energy of 150 eV.

In Fig. 1 (a) a LEED pattern of the Au nanowire decorated Si(553) surface is shown. Clear integer order spots reflect the  $(1 \times 1)$  unit cell of the underlying Si(553) surface (as indicated in Fig. 1 (a) as grey shaded rhomboid) with dimensions of  $2\pi/3.84 \text{ \AA} \times 2\pi/14.8 \text{ \AA}$  along the  $[1\bar{1}0]$  and  $[3\bar{3}\bar{1}0]$  crystallographic orientations. The corresponding real space unit cell can either be interpreted as primitive  $(1 \times 1)$  cell or as a *centered* unit cell with dimensions of  $3.84 \text{ \AA} \times 2 \cdot 14.8 \text{ \AA}$ , thus reflecting the underlying rectangular symmetry of the Si(553) surface. The next dominant feature of the LEED pattern is the streaklike intensity along the  $[3\bar{3}\bar{1}0]$  direction. These streaks at half way between the integer order spots arise from the strict  $\times 2$  periodicity of the Au dimers along the wires.

The most intriguing feature of the diffraction pattern, however, is intensity located at  $1/3$  and  $2/3$  positions in between the rows of integer order spots, reflecting  $\times 3$  periodicity along the steps. Such intensity has also been observed in LEED patterns of previous experiments as “streaks”<sup>12,14,21</sup>. This is consistent with the *original* structure model which explains this tripled periodicity through partial charge transfer from the Au atoms to the Si dangling bonds at the step edges, leaving every third Si step edge atom fully spin polarized. Here we observe a clear series of only slightly elongated spots instead of “streaks”. To emphasize this, Fig. 2 shows a LEED intensity line profile taken along the  $[3\bar{3}\bar{1}0]$  at the  $-2/3$

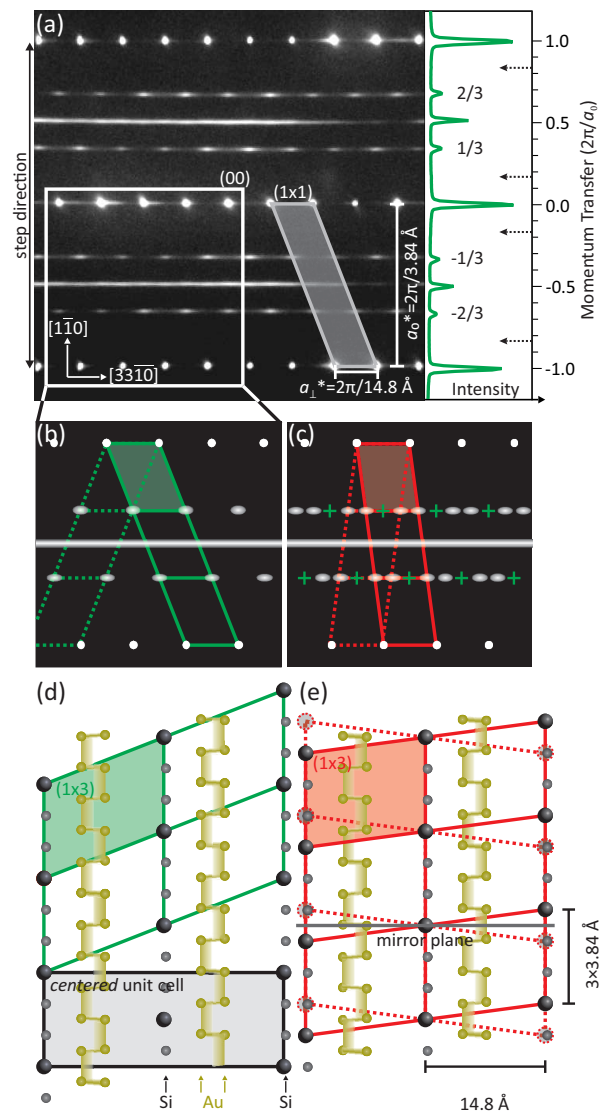


Figure 1. (a) LEED pattern of the Si(553)-Au surface taken at 150 eV and  $T = 80 \text{ K}$ . The primitive  $(1 \times 1)$  reciprocal unit cell is indicated by a grey rhomboid. Half way between the rows of sharp integer order spots streaks are found originating from dimer Au rows along the terraces. Located at  $1/3$  and  $2/3$  positions slightly elongated spots from the tripled periodicity of the Si step edge atoms indicate a clear long-range ordering. The integrated line profile taken along the  $[1\bar{1}0]$  direction (right side of the diffraction pattern) does not show any intensity indicating  $\times 6$  periodicity (dashed arrows). (b) Sketch of the diffraction pattern with  $(1 \times 3)$  unit cells (green solid line). The green dashed lines depict the super-imposed mirror-domain resulting in coinciding diffraction spots. (c) Expected diffraction pattern and unit cells of the *original* structure proposed by Erwin *et al.*<sup>6</sup> with expected diffraction spot positions indicated by grey ovals. Green crosses mark the positions of experimentally found diffraction spots. (d) New structure model with modified primitive (green rhomboids) or *centered* unit cell (black rectangular), respectively. (e) *Original* structure model (solid red line) superimposed with mirror domain (dashed red line). The Si step edge atoms are indicated in grey and Au atoms as yellow spheres. Dimerization is indicated by the shaded yellow lines.

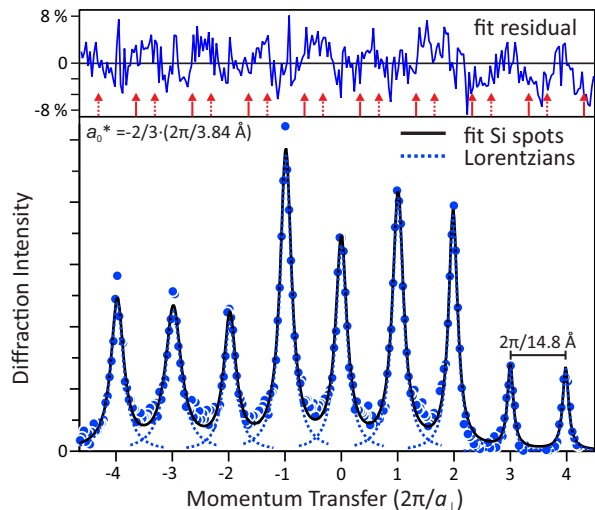


Figure 2. Intensity line profile of the diffraction pattern at  $-2/3$  position along the  $[33\bar{1}0]$  direction. The clearly peaked structure (blue dots) with the same equidistant periodicity as the underlying substrate ( $a_{\perp}^* = 2\pi/14.8 \text{ \AA}$ ) is fitted by a series of Lorentzian functions (dashed and solid lines) and a constant background intensity. In the upper part of the figure the residual of the fit is depicted. The red arrows point to the positions indicative for the two equivalent structures sketched in Fig. 1 (e).

position in the Brillouin zone. Clear spots with low constant background intensity are separated by  $2\pi/14.8 \text{ \AA}$ , thus showing the same periodicity as the underlying substrate. Both findings are direct evidence for long-range ordering of the  $\times 3$  periodicity of the Si step edge atoms perpendicular to the steps. This is in clear contrast to the Au dimer rows in between, which do not show such a spot-like intensity, thus exhibiting no fixed phase correlation between neighboring Au-chains. This is in clear contrast to the Au dimer rows in between, which do not show such a spot-like intensity, thus exhibiting no fixed phase correlation between neighboring Au-chains. This leads to such large broadening of the spots along the  $[33\bar{1}0]$  direction that only streaks are visible.

In Fig. 1 (e) the most important features of the real space structure of the *original* model are sketched. The dimerized double-strand Au rows, which are the origin of the half order streaks, are shown in yellow. Every third Si step edge atom with its unoccupied orbital is highlighted by a larger grey circle. From the position of the  $1/3$  and  $2/3$  spots in reciprocal space we are now able to unambiguously determine the geometry of the  $(1 \times 3)$  unit cell spanned by the Si step edge atoms with unoccupied orbitals. Taking the  $\times 3$  periodicity of the Si step edge atoms as a commonly accepted structural element, then the geometry of the  $(1 \times 3)$  unit cell only depends on the correlation of the Si step edge atoms with unoccupied orbitals between neighboring steps. There are three possible lateral translational vectors to define the correlations of Si step edges in neighboring steps,

spanning the primitive unit cells.

In the *original* model these Si atoms of the neighboring steps are shifted upwards by half of a substrate unit cell ( $1/2 a_0$ ) along the step direction. The corresponding series of reciprocal space unit cells is indicated by red solid lines in Fig. 1 (c). Performing a mirror operation with a mirror plane along the  $[33\bar{1}0]$  direction results in the geometry shown in Fig. 1 (e) with the  $(1 \times 3)$  unit cells pictured in dashed red lines. The corresponding reciprocal unit cell is indicated by dashed red lines in Fig. 1 (c). We expect diffraction spots at the positions indicated by the grey ovals which do not coincide, but exhibit alternating separations of  $1/3 a_{\perp}^*$  and  $2/3 a_{\perp}^*$  between each other. Obviously the position of the experimentally observed diffraction spots (marked by green crosses) do not match the grey ovals predicted for the *original* unit cell geometry.

The third possible geometry results from a lateral shift of  $3/2 a_0$  as indicated in green lines in Fig. 1 (d). The geometry of this structure remains unchanged after mirror operation with a mirror plane perpendicular to the steps. The inherent higher symmetry of this primitive unit cell manifests in the possibility to describe it with a centered geometry, i.e., a *centered* unit cell. The corresponding series of  $(1 \times 3)$  reciprocal unit cells is shown in Fig. 1 (b) in green lines and exactly fits the positions of the measured diffraction spots. From the spot profile shown in Fig. 2 we can exclude any significant presence of the structure elements sketched in Fig. 1 (e). The spot profile of the equidistant series of  $1/3$  order spots has been fitted by a series of Lorentzian functions, describing a geometric distribution of domains with finite correlation length<sup>28,29</sup> perpendicular to the steps of  $\Gamma \approx 10 \text{ nm}$ . The residuum between the fit and the experimental data is shown in the upper part of Fig. 2(a). From the absence of remaining intensity at the positions (indicated by dashed and solid red arrows) expected for the two other structural models [Fig. 1 (e)] we can conclude that the entire surface exhibits the *centered* type unit cell as presented in Fig. 1 (d).

The new *centered* structure is also present in the STM image shown in Fig. 3. For the area shown in zoom #1 the *centered* registry is preserved over a distance of eight chains consistent with the correlation length extracted from the SPA-LEED line profiles. Zoom #2 depicts two antiphase translational domains (green unit cells) separated by a linear domain boundary which locally exhibits the *original* structure (red unit cell). Note, that the STM data presented in Fig. 3 provides a significant higher correlation length compared to previous STM studies<sup>9</sup>, in which the new registry is only observed across three chains. This was achieved by improved UHV conditions leading to a decreased defect concentration which significantly reduces the number of domain boundaries.

For the combination of a  $\times 3$  periodicity of the Si step edge atoms and a  $\times 2$  periodicity of the Au wires, respectively, the smallest unit cell along the steps must exhibit a  $\times 6$  periodicity. We therefore would expect intensity



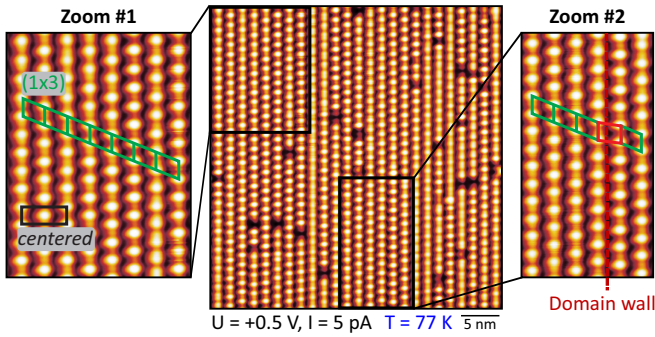


Figure 3. STM image of the Si(553)-Au surface at 77 K depicting the empty states. The tunneling bias was chosen  $U = +0.5$  V to highlight the  $\times 3$  periodicity of the Si step edge atoms with partially filled dangling bonds. Zoom #1 shows a well ordered eight chain wide area of the *centered* unit cell. Zoom #2 depicts two ordered *centered* domains separated by a linear domain wall, locally exhibiting the *original* structure.

at  $1/6$  and  $5/6$  positions in the diffraction pattern. In the right inset of Fig. 1 (a) the line profile of the diffraction pattern after integration along the  $[3\bar{3}10]$  direction is shown. It does not show any traces of peaks at the expected positions: in LEED, which is sensitive both to the electron density and the position of the nuclei, we do not observe a  $\times 6$  periodicity along the steps. From this, we have to conclude that the structural elements of the  $\times 3$  periodicity of the Si step edge atoms and of the  $\times 2$  periodicity of the Au rows act as independent scatterers during diffraction. Any mutual interaction between Au and Si chain, respectively, can not be detected within the accuracy of our LEED experiment.

The presence of spots instead of streaks in diffraction implies long-range order perpendicular to the steps and thus leads to an important conclusion: there is a significant interaction between the Si step edges despite their substantial separation of  $14.8$  Å. We propose that this interaction is primarily Coulombic, and arises from the Madelung energy associated with the interaction of the charges on the step edges. These charges can be determined using the electron configurations of the step-edge dangling bonds. Two out of three of these dangling bonds are each fully occupied by two spin-paired electrons, while every third dangling bond has just one electron (and is therefore fully spin polarized<sup>6</sup>). Hence the average occupancy of  $(5/3)e$  is modulated by a CDW consisting of a deficit of  $(2/3)e$  on every third atom and an excess  $(1/3)e$  on each of the other two. By assuming perfect lateral ordering of these charges on an infinite flat surface the total electrostatic energy of the CDW can then be written as  $E = -\alpha q^2/a_0$ , where  $\alpha$  is the Madelung constant,  $q = (2/3)e$  is the charge modulation, and  $a_0$  is the maximum separation between neighboring charges along a row. The Madelung constants were calculated by directly summing the electrostatic interaction energies over  $N$  shells of the surface unit cells.

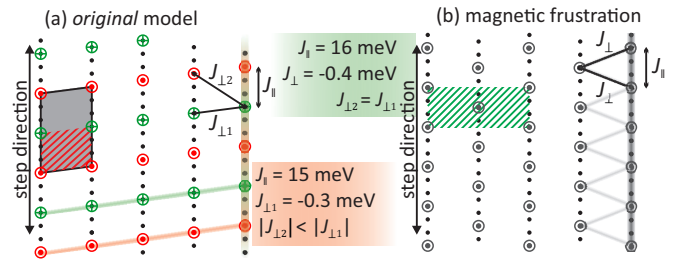


Figure 4. Schematics of possible spin ordering. (a) For the *original* unit cell antiferromagnetic coupling along and ferromagnetic coupling perpendicular lead to magnetic long-range ordering. Spin polarized Si step edge atoms are marked with red circles and green crosses indicating local spin up and down polarization. The structural unit cells are indicated by dashed polygons. The smallest possible magnetic unit cell is marked by black lines. (b) In the modified unit cell the magnetic intra- and interchain nearest-neighbor coupling lead to frustrated interaction, suppressing any magnetic order.

This procedure converges with  $N$  sufficiently quickly in 2D. The resulting total energy was extrapolated to infinite  $N$  by fitting the finite- $N$  results to a power series in  $1/N$  and taking the limit (accuracy  $1 : 10^4$ ). We find that the Madelung constant for the new unit cell,  $\alpha_{\text{centered}} = 1.6488$ , is indeed slightly larger than for the *original* unit cell,  $\alpha_{(1 \times 3)} = 1.6475$ . This difference corresponds to an energy preference of  $2.1$  meV per spin for the new unit cell. To check this estimate we performed DFT calculations, using methods detailed in Ref. 6, comparing the total energies of the two geometries. The new geometry is favored by  $1.6$  meV per spin, in excellent agreement with the estimate based on Madelung energies.

The *centered* geometry of the unit cell also has implications for the magnetism of the local spin moments on every third Si step edge atom. Density-functional calculations for the *original* structure in Ref. 6 found that the spins are antiferromagnetically coupled along the step edges. For a strictly 1D spin chain quantum fluctuations prevent any magnetic ordering<sup>30</sup>. In the real system, however, additional couplings along other dimensions, in particular between neighboring step edges, will stabilize long-range order at sufficiently low, but finite temperatures. For example, if mapped onto a nearest-neighbor Heisenberg model the calculations for the *original* structure yield an exchange constant along the chains of  $J_{\parallel} = 15$  meV, while the coupling between nearest spins on neighboring chains is found to be ferromagnetic and of magnitude  $J_{\perp 1} = -0.3$  meV (see Fig. 4 (a)). The exchange constant to the next-nearest neighbor spin on adjacent chains,  $J_{\perp 2}$ , had not been calculated, but is expected to be considerably smaller than  $J_{\perp 1}$  due to the larger spin-spin separation. In this situation a complex, overall antiferromagnetic ground state would be assumed. This drastically changes in the new structure reported here:  $J_{\perp 1}$  and  $J_{\perp 2}$  are now degenerate [ $J_{\perp}$ , see Fig. 4 (b)] leading to magnetic frustration and hence the

suppression of magnetic order, independent of the sign of  $J_{\perp}$ . This situation has theoretically been studied in much detail within the anisotropic triangular Heisenberg spin- $\frac{1}{2}$  model (e.g. Ref. 31). Its phase diagram is controlled by the single parameter  $|J_{\perp}|/J_{\parallel}$ , which for values  $< 0.8$  leads to a 2D quantum spin liquid ground state. Such exotic phases have previously been reported for quasi-2D bulk anorganic<sup>32</sup> and organic materials<sup>33</sup>. In the new structure model the exchange constant along the chains is calculated to be  $J_{\parallel} = 16$  meV and perpendicular to the steps  $J_{\perp} = -0.4$  meV, respectively. These values differ only slightly compared to the *original* model, but provide an additional contribution to the energy lowering of the *centered* geometry by the larger spin interaction. For the new structure a parameter  $|J_{\perp}|/J_{\parallel} = 0.025$  is obtained. This places the magnetic ground state of the local spins in the Si(553)-Au system deep in the 2D spin liquid regime<sup>31</sup>. In the mentioned bulk materials the spin liquid properties have been identified through the temperature dependence of the magnetic susceptibility. Measuring this quantity for the surface spins in Si(553)-Au represents an experimental challenge, but could possibly be achieved by x-ray magnetic circular dichroism (XMCD) experiments at the Si K- and L-edges<sup>34</sup>.

In summary, high resolution SPA-LEED, STM and DFT were employed to study the geometric structure of the Si(553)-Au system, which exhibits self-organized 1D Au atom rows on highly ordered Si step arrays separated by 14.8 Å. These double-strand Au rows are dimerized

and therefore show a double periodicity along the steps. The step edges are built by single honeycomb graphitic strips of Si atoms exhibiting a pronounced  $\times 3$  periodicity along the steps. Both structural elements can easily be separated in the diffraction pattern and had been observed as weak streaklike intensity in earlier studies. Scrutinizing with SPA-LEED's superior signal-to-noise ratio we were able to detect individual diffraction spots instead of a streaked intensity. This made it possible to unambiguously determine the geometry of the surface unit cell spanned by the spin polarized Si step edge atoms, i.e., a *centered* geometry of the unit cell. As a consequence, the magnetic exchange interactions are found to be frustrated between neighboring spin chains, which in the framework of the anisotropic triangular Heisenberg model would stabilize an exotic 2D quantum spin liquid.

## ACKNOWLEDGMENTS

Financial support from the DFG FOR1700 research unit "metallic nanowires on the atomic scale: Electronic and vibrational coupling in real world systems" is gratefully acknowledged. This work was partly supported by the Office of Naval Research through the Naval Research Laboratory's Basic Research Program (SCE). Computations were performed at the DoD Major Shared Resource Center at AFRL.

\* bernd.hafke@uni-due.de

<sup>1</sup> P. C. Snijders and H. H. Weitering, Rev. Mod. Phys. **82**, 307 (2010).  
<sup>2</sup> F. Himpfel, K. Altmann, R. Bennwitz, J. Crain, A. Kirakosian, J. Lin, and J. McChesney, J. Phys.: Condens. Matter **13**, 11097 (2001).  
<sup>3</sup> H. Yeom, S. Takeda, E. Rotenberg, I. Matsuda, K. Horikoshi, J. Schaefer, C. Lee, S. Kevan, T. Ohta, T. Nagao, *et al.*, Phys. Rev. Lett. **82**, 4898 (1999).  
<sup>4</sup> P. Segovia, D. Purdie, M. Hengsberger, and Y. Baer, Nature **402**, 504 (1999).  
<sup>5</sup> J. Aulbach, S. C. Erwin, R. Claessen, and J. Schäfer, Nano Lett. **16**, 2698 (2016).  
<sup>6</sup> S. C. Erwin and F. J. Himpfel, Nat. Commun. **1**, 58 (2010).  
<sup>7</sup> K. Biedermann, S. Regensburger, T. Fauster, F. Himpfel, and S. Erwin, Phys. Rev. B **85**, 245413 (2012).  
<sup>8</sup> P. C. Snijders, P. S. Johnson, N. P. Guisinger, S. C. Erwin, and F. J. Himpfel, New J. Phys. **14**, 103004 (2012).  
<sup>9</sup> J. Aulbach, J. Schäfer, S. C. Erwin, S. Meyer, C. Loho, J. Settlein, and R. Claessen, Phys. Rev. Lett. **111**, 137203 (2013).  
<sup>10</sup> I. Song, J. S. Goh, S.-H. Lee, S. W. Jung, J. S. Shin, H. Yamane, N. Kosugi, and H. W. Yeom, ACS Nano **9**, 10621 (2015).  
<sup>11</sup> J. Crain, A. Kirakosian, K. Altmann, C. Bromberger, S. Erwin, J. McChesney, J.-L. Lin, and F. Himpfel, Phys. Rev. Lett. **90**, 176805 (2003).  
<sup>12</sup> J. R. Ahn, P. G. Kang, K. D. Ryang, and H. W. Yeom,

Phys. Rev. Lett. **95**, 196402 (2005).

<sup>13</sup> I. Song, D.-H. Oh, H.-C. Shin, S.-J. Ahn, Y. Moon, S.-H. Woo, H. J. Choi, C.-Y. Park, and J. R. Ahn, Nano Lett. **15**, 281 (2015), <http://dx.doi.org/10.1021/nl503558g>.  
<sup>14</sup> S. Hasegawa, J. Phys.: Condens. Matter **22**, 084026 (2010).  
<sup>15</sup> P. C. Snijders, S. Rogge, and H. H. Weitering, Phys. Rev. Lett. **96**, 076801 (2006).  
<sup>16</sup> H. Okino, I. Matsuda, S. Yamazaki, R. Hobara, and S. Hasegawa, Phys. Rev. B **76**, 035424 (2007).  
<sup>17</sup> S. Ghose, I. Robinson, P. Bennett, and F. Himpfel, Surf. Sci. **581**, 199 (2005).  
<sup>18</sup> K.-D. Ryang, P. G. Kang, H. W. Yeom, and S. Jeong, Phys. Rev. B **76**, 205325 (2007).  
<sup>19</sup> T. Takayama, W. Voegeli, T. Shirasawa, K. Kubo, M. Abe, T. Takahashi, K. Akimoto, and H. Sugiyama, e-J. Surf. Sci. Nanotechnol. **7**, 533 (2009).  
<sup>20</sup> W. Voegeli, T. Takayama, T. Shirasawa, M. Abe, K. Kubo, T. Takahashi, K. Akimoto, and H. Sugiyama, Phys. Rev. B **82**, 075426 (2010).  
<sup>21</sup> H. W. Yeom, S. W. Jung, J. S. Shin, J. Kim, K. S. Kim, K. Miyamoto, T. Okuda, H. Namatame, A. Kimura, and M. Taniguchi, New J. Phys. **16**, 093030 (2014).  
<sup>22</sup> M. Krawiec, Phys. Rev. B **81**, 115436 (2010).  
<sup>23</sup> S. Polei, P. Snijders, S. Erwin, F. Himpfel, K. Meiwes-Broer, and I. Barke, Phys. Rev. Lett. **111**, 156801 (2013).  
<sup>24</sup> S. Polei, P. C. Snijders, K.-H. Meiwes-Broer, and I. Barke, Phys. Rev. B **89**, 205420 (2014).  
<sup>25</sup> P. Kury, R. Hild, D. Thien, H.-L. Günter, F.-J. Meyer zu

- Heringdorf, and M. Horn-von Hoegen, *Rev. Sci. Instrum.* **76**, 083906 (2005).
- <sup>26</sup> U. Scheithauer, G. Meyer, and M. Henzler, *Surf. Sci.* **178**, 441 (1986).
- <sup>27</sup> M. Horn-von Hoegen, *Z. f. Kristallographie* **214**, 591 (1999).
- <sup>28</sup> M. Henzler, *Surf. Sci.* **73**, 240 (1978).
- <sup>29</sup> C. Lent and P. Cohen, *Surf. Sci.* **139**, 121 (1984).
- <sup>30</sup> N. D. Mermin and H. Wagner, *Phys. Rev. Lett.* **17**, 1133 (1966).
- <sup>31</sup> S. Yunoki and S. Sorella, *Phys. Rev. B* **74**, 014408 (2006).
- <sup>32</sup> R. Coldea, D. Tennant, A. Tsvetik, and Z. Tylczynski, *Phys. Rev. Lett.* **86**, 1335 (2001).
- <sup>33</sup> Y. Shimizu, K. Miyagawa, K. Kanoda, M. Maesato, and G. Saito, *Phys. Rev. Lett.* **91**, 107001 (2003).
- <sup>34</sup> C. Antoniak, H. Herper, Y. Zhang, A. Warland, T. Kachel, F. Stromberg, B. Krumme, C. Weis, K. Fauth, W. Keune, *et al.*, *Phys. Rev. B* **85**, 214432 (2012).